Empirical model of total internal reflection from highly turbid media

K. G. Goyal,[1] M. L. Dong,[1] V. M. Nguemaha,[1] B. W. Worth,[1] P. T. Judge,[1] W. R. Calhoun,[2] L. M. Bali,[1] and S. Bali[1,*]

[1]*Department of Physics, Miami University, Oxford, Ohio 45056-1866, USA*

[2]*U.S. Food and Drug Administration, Center for Devices and Radiological Health, Silver Spring, Maryland 20993, USA*

**Corresponding author: balis@miamioh.edu*

Received May 29, 2013; revised October 9, 2013; accepted October 10, 2013;
posted October 18, 2013 (Doc. ID 191208); published November 14, 2013

We demonstrate, to the best of our knowledge, a first accurate empirical model for reflectance measurements from highly turbid media over the full range of incident angles, i.e., for reflectivity values going from unity in the total internal reflection regime to nearly zero when almost all the light is transmitted. Evidence that our model is accurate is provided by extraction of the particle size, followed by independent verification with dynamic light scattering. Our methodology is in direct contrast with the prevalent approach in turbid media of focusing on only the critical angle region, which is just a small subset of the entire reflectance data.

OCIS codes: (120.0280) Remote sensing and sensors; (170.7050) Turbid media; (290.7050) Turbid media; (280.1415) Biological sensing and sensors; (120.5820) Scattering measurements; (260.6970) Total internal reflection.
http://dx.doi.org/10.1364/OL.38.004888

Light propagation in turbid media, i.e., colloidal suspensions of particles comparable in size to the optical wavelength, has been carefully explored over the past several decades due to this topic's fundamental importance in science and technology. Regardless of the particle size and density, the concept of an effective refractive index for turbid media is established to be meaningful [1]. Remarkably, a verifiably accurate determination of the complex refractive index of a highly turbid medium has, to date, eluded researchers. This is because transmission-based methods fail in highly turbid media owing to extreme attenuation, and refractive index determination is typically based on the measurement of total internal reflection (TIR) from the sample surface. To the best of our knowledge, there has not been a single case reported where the entire reflectance data from the surface of a highly turbid medium, spanning both TIR and non-TIR regimes, has been accurately described by any theoretical model, though some progress was made recently [2].

Previous attempts to accurately model the reflectance data and measure the complex refractive index suffered from at least one of three important shortcomings: first, extraneous fitting parameters were introduced to account for hard-to-estimate factors such as multiple scattering in the turbid medium [4–6], or, in the case of [7], the volume fraction of the suspended particles, even though the goal is to determine just two parameters: the real and imaginary refractive index. This resulted in overfitting of the data. Second, fitting was performed of only the critical angle region [2,8,9] (e.g., reflectance data only between 1 and 0.75 was fitted while important information between 0 and 0.75 was simply ignored [2]). Third, no reliable reference data exist for the medium investigated (e.g., milk-cream [2,8], intralipid [9]).

Furthermore, reliable *in situ* particle sizing is a long-sought goal in colloidal science. Standard sizing methods such as optical microscopy and dynamic light scattering (DLS) are not *in situ* since they require heavy dilution of turbid samples in order to avoid multiple scattering. Theoretical models enabling *in situ* measurement of complex refractive index are desired, as one may extract particle size from the index using Mie calculations [10].

Rigorous theoretical frameworks for light propagation in turbid media carry formidable computational/time cost [11], necessitating a search for an empirical, simpler model. However, the most widely used empirical method of "differentiation," which associates the point of maximum slope of the reflectance-versus-incident-angle curve with an effective critical angle [4,6,8,9], is significantly inaccurate even after error correction is attempted [12].

In this letter, we demonstrate, for the first time, a verifiably accurate method for *in situ* (i.e., no sample dilution) measurement of the complex refractive index and particle size in highly turbid media. Our method relies upon an empirical model of TIR in turbid media, first proposed by us in [2], which quantitatively accounts for the loss in TIR intensity during angle-dependent penetration by incident light into the medium. We achieved this by introducing in our model the concept of an angle-dependent imaginary component of refractive index. Verification is provided by using our model to extract the particle size via Mie calculation, and finding excellent agreement with independent DLS size measurements. Note that while DLS is unreliable in colloidal suspensions of unknown composition owing to the requirement that the refractive index of the dispersion medium be known, DLS is reliable in well-characterized stable suspensions. Our samples comprise aqueous monodisperse (i.e., particles of well-defined singular size) solutions of polystyrene microspheres. However, in DLS, dilution is necessary in order to satisfy a key assumption behind Mie theory; namely, that no multiple scattering events occur. On the other hand, in our experiments this assumption is well-satisfied despite our use of undiluted highly turbid samples. We test our model extensively in solutions of different particle sizes and concentrations.

Our experimental setup, outlined in Fig. 1(a), consists of a turbid sample of refractive index n_s placed on a glass prism of known refractive index, illuminated by a divergent p polarized beam of ~6 μW at 660 nm from a diode laser pigtailed to a single-mode fiber. The use

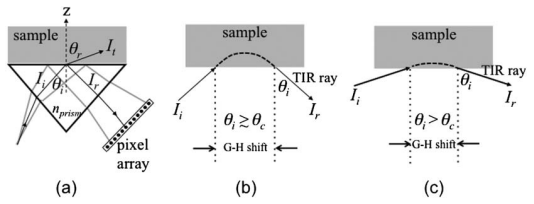

Fig. 1. (a) Prism-sample interface for measuring $I_r/I_i(\theta_i)$ with a divergent incident beam. For low values of θ_i, light mostly refracts through (I_t), but TIR occurs for higher values. (b) and (c) depict angle-dependent penetration in TIR for transparent samples. The penetration is maximum at the critical angle. In a turbid medium, the picture is similar, but θ_c is not defined. G-H, Goos–Hänchen.

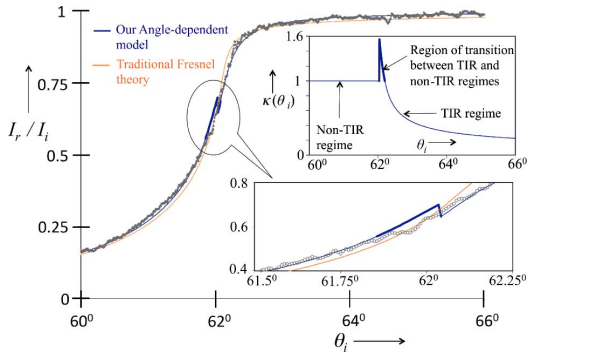

Fig. 2. Reflectance data (1000 datapoints) for aqueous solution of polystyrene spheres (dia 0.356 ± 0.014 μm). Solid lines are theoretical fits; dots are data. Both the angle-dependent model [dark blue; see text for explanation of spike (bold)] and traditional Fresnel theory (light orange) fit data closely, yet only one is correct.

of a divergent beam eliminates the need for angular scanning, suppressing mechanical noise. The design is essentially identical to that described in detail earlier [2,13], except that in [2] only a small subset of the entire reflectance data was measured, leaving the authors in no position to perform accurate particle sizing, and in [13] only transparent samples were studied.

For turbid media, n_s is complex $n_s = n_r + in_i$, where the real part n_r arises from the bending of light at the interface, and the imaginary part n_i is related to the turbidity through the relation $\alpha = 2n_i\omega/c$. Here α is the attenuation coefficient given by $I(z) = I_0 \exp(-\alpha z)$; $I(z)$ is the intensity of a light beam propagating through the medium, I_0 is the incident intensity at $z = 0$, ω is the laser frequency, and c is the speed of light in a vacuum. We designate $\alpha \geq 200$ cm^{-1} "highly turbid" because conventional transmission-based imaging methods typically fail, and one must use reflectance-based methodologies [2].

In the traditional approach to modeling the refractive index of turbid media, one simply allows n_s to be complex in Fresnel theory. Our approach is to use a modified Fresnel theory we introduced in [2] that incorporates angle-dependent penetration of the incident light into the medium (which forms the basis for the well-known Goos–Hänchen shift [14]) as seen in Figs. 1(b) and 1(c). This yields an angle-dependent n_i, i.e., $n_i(\theta_i) = n_i\kappa(\theta_i)$ which is no longer a constant as is assumed traditionally. The form of the angular factor κ is plotted in Fig. 2, top inset. In the non-TIR regime n_i is a constant, and κ is unity for all angles, just as in the usual case of normal incidence. But in the TIR regime κ is given by [2]

$$\kappa(\theta_i) = \left(4\pi n_{\text{prism}}\sqrt{(M-L)/2}\right)^{-1}, \qquad (1)$$

which is a smoothly varying downward-sloping function (the unseemly spike in the TIR–non-TIR transition region is explained later). Here $L = [(n_r^2 - n_i^2)/n_{\text{prism}}^2] - \sin^2\theta_i$, $M = \sqrt{P^2 - 2L\sin^2\theta_i - \sin^4\theta_i}$, and $P = (n_r^2 + n_i^2)/n_{\text{prism}}^2$. Equation (1) for the angle-dependent component of $n_i(\theta_i)$ is just the ratio of the penetration depth to the optical wavelength. The angle-dependent penetration depth of an evanescent wave in TIR is well known in transparent media [15–17]; a ray picture of this angle-dependent penetration is depicted by invoking the Goos–Hänchen shift [14] of the exit ray relative to the incident ray in Figs. 1(b) and 1(c). However, Eq. (1) gives the corresponding explicit expression for the penetration depth (divided by λ) in a turbid medium. The evanescent wave corresponding to each plane-wave component of our divergent beam scatters inside the turbid medium [16,18]. The scattering-induced intensity loss in each evanescent wave varies with the wave's penetration, leading to an angle-dependent loss in TIR intensity [expressed by the angle-dependent n_i in Eq. (1)].

Figure 2 shows I_r/I_i curves as a function of incident angle θ_i for a highly turbid aqueous solution of latex microspheres. Each datapoint in the figure is represented by a gray dot, which is an average over 100 measurements. The size of the error bar on each datapoint is smaller than the size of the gray dot. First we measure the reflected intensity profile with no sample [this yields $I_i(\theta_i)$ provided TIR occurs at the prism-air interface for all θ_i]. The measurement is repeated 100 times, and an average profile is generated and stored—this process takes 10 s. Next the sample is placed on top of the prism, and the average reflected intensity profile is similarly generated [this yields $I_r(\theta_i)$; we choose the prism material and angle so that the TIR non-TIR transition occurs at some angle within the range of angles subtended by the divergent beam]. Finally, the ratio of the two profiles is taken. We checked that the gravity-induced sedimentation during the time taken to generate an intensity profile, such as in Fig. 2, is negligible. The sedimentation velocity is proportional to the square of the particle size, acceleration due to gravity, and the difference in densities between polystyrene and water, and inversely proportional to the viscosity of water [19]. We estimate the sedimentation velocity for the largest particles (dia = 0.5 μm) used in our experiment to be 0.04 nm/s, meaning that the particles move ≤1 nm during the time taken to measure the intensity profile shown in Fig. 2, which is a negligible fraction of the optical wavelength.

The light-orange and dark-blue curves in Fig. 2 are best possible fits obtained by traditional Fresnel theory (denoted by F from here on) and by our angle-dependent model [denoted AM, given by Eq. (1)], respectively. Each fit is optimized by minimizing its mean-square-deviation (MSD). Note that Eq. (1) describes a new angle-dependent n_i in terms of M and L that themselves depend

Table 1. AM and F Models Yield Different Particle Sizes

Model	n_r	α (cm^{-1})	MSD $\times 10^{-4}$	Particle Diameter (μm)
AM	1.33740	379	1.51	0.387 ± 0.010
F	1.33837	193	2.64	0.254 ± 0.007

on n_i. Therefore, we start with a constant-value best-guess for n_r and n_i in the expressions for L, M, and P, then construct an angle-dependent $n_i(\theta_i)$ from Eq. (1). Next we substitute this new $n_i(\theta_i)$ into the Fresnel reflection coefficient and perform again a best fit of I_r/I_i to the data; the only two fitting parameters we adjust are the first best-guess values used for n_r and n_i. In a few iterations, we obtain the best possible fit yielding our final n_r and n_i (or α) values.

Table 1 shows that even though both the F and AM models fit the data in Fig. 2 almost equally well, the two models yield significantly different values for α and particle size (and also n_r since a difference of 0.001 is significant for most applications).

Which model should we trust? In answer, we used particle sizing by DLS as the benchmark for comparison with each model's sizing predictions [20]. DLS is especially reliable when sizing in monodisperse stable aqueous solutions: errors are minimized since the refractive index and viscosity of deionized water and refractive index of polystyrene are well-known. In order to determine particle size from the F and AM fits, we use a Mie numerical calculation [10] at 660 nm, which outputs α and requires as input parameters certain well-known quantities such as the refractive index of deionized water at the experiment temperature (25°C in our case), the real and imaginary refractive indices of polystyrene microspheres and density of polystyrene [7,21], and microsphere concentration (determined from weight/volume supplied by manufacturer). The particle size appears as an input parameter and is iteratively adjusted until α yielded by the Mie program agrees with α predicted by each model. Note that we have made the usual assumption of spherical particle shape for application of Mie theory.

Note that in our experiment, the optical depth (OD $= \alpha$ times the sample length traversed), is ≤ 0.04 even for our most highly turbid sample ($\alpha = 578$ cm^{-1} in Table 2) owing to the evanescent light merely penetrating on the order of λ into the medium [see Figs. 1(b) and 1(c)]. Thus the probability that an incident photon is scattered once is ≤ 0.04, and the probability of multiple scattering is at least the square of that. The single scatterings cause the reflectance to decrease below unity in the TIR regime for a highly turbid medium. However, the probability for multiple scattering in our experiment is negligible [18], thus validating our use of Mie theory for the evaluation of the attenuation α. In order to estimate the range of turbidities for the validity of our model, we note that the simple probability-based argument above may be used only as long as the OD is significantly less than unity. For example, for turbidities $\geq 10,000$–$15,000$ cm^{-1}, the OD for the thin λ deep penetration layer approaches unity, and the interpretation of OD as a probability breaks down. Multiple scattering within the penetration depth will occur, precluding the use of Mie theory. On the other hand, our lowest turbidity data (first row, Table 2) indicate that for $\alpha \leq 5$ cm^{-1}, there is no significant difference between predictions from our model and from traditional Fresnel theory.

Table 2 presents particle-size measurements for five different particle sizes and several different turbidities (i.e., concentrations). Error bars on particle size were provided by the manufacturers for just two samples: the 0.054 μm spheres were specified to have error ±0.007%, and the 0.356 μm spheres ±0.014%. Residual error in DLS values (Malvern Instruments Zetasizer) from imprecision in temperature measurement (leads to error in viscosity) is ≤1–2%, confirmed by multiple measurements on samples with the same particle size but different concentrations (see the 0.2 μm data in Table 2). Statistical errors from multiple measurements result in error bars on the particle size measurements using the AM and F models: They were found to range from a minimum of ±0.001 μm in the case of the 0.054 μm spheres to a maximum of ±0.018 μm for the 0.1 μm spheres. Column 6, Table 2 shows the particle sizes extracted from our AM model to be in good agreement with DLS; the discrepancy is less than 10% in all cases. This implies the α values extracted by AM are correct as well (as should be the n_r values, which we do not show for brevity). By contrast, it is only for the sample with the lowest turbidity (and lowest particle size) that particle sizing from F theory (Column 7) has similar agreement with DLS as our AM model. For all other samples, disagreement of F with DLS is significantly large, tending to grow with rising turbidity and/or particle size, exceeding 40% for 0.5 μm particles at $\alpha_{AM} = 578$ cm^{-1}. Note that F theory's prediction for α in this case differs from AM by more than a factor of two. Interestingly, from the last column in Table 2, we see that, despite yielding inaccurate particle sizes, the traditional F model actually fits the data better for half the samples, i.e., the ratio of the

Table 2. Comparison of Particle-Sizing by AM and F Models for Different Particle Sizes and Concentrations (Size Errors in Columns 6 and 7 are Calculated Relative to the DLS Sizes in Column 3)

Manu. Size (μm)	Vol. Frac. (%)	DLS Size (μm)	α AM (cm^{-1})	α F (cm^{-1})	Size Error AM	Size Error F	MSD Ratio AM/F
0.054	2.48	0.059	4	6	−8%	+7%	1.1
0.1	0.95	0.124	17	30	+2%	+30%	1.0
0.2	2.38	0.185	91	82	−6%	−10%	1.3
0.2	4.76	0.185	223	146	+3%	−14%	1.4
0.2	9.52	0.187	475	247	+5%	−21%	1.2
0.356	2.51	0.385	379	193	+0.5%	−34%	0.6
0.5	0.95	0.477	172	109	−7%	−31%	0.5
0.5	2.86	0.477	578	252	+3%	−42%	0.2

MSD value for our AM model to the MSD value for traditional F theory exceeds unity in four of the samples with smaller particle size. This proves that "goodness of fit" as a sole criterion for validity of a model is misleading. Nevertheless, Table 2 shows that with rising turbidity and particle size the AM model yields more accurate particle sizing than F, and fits the data better. An MSD ratio of 0.6 for the 0.356 μm sample means AM fits the data 2X better than F, visibly so already in Fig. 2.

The insets in Fig. 2 underline the importance of fitting the *entire* reflectance data-curve and elucidate the origin of the unseemly spike, or glitch, in the theoretical AM fit, as explained immediately below. The top inset illustrates how we switch between a constant value for $n_i(\theta_i)$ in the non-TIR regime and a downward-sloping angle-dependent value in the TIR regime. But in highly turbid media, where there exists no critical angle, how does one decide at which specific angle to apply this switch? In transparent media, the critical angle is unambiguously the angle at which $L(\theta_i) = 0$. Therefore, as our initial guess, we choose the location of the switch as the angle at which $L(\theta_i)$ changes sign from positive (non-TIR regime) to negative (TIR). We now perform a best fit of I_r/I_i to the data by iteratively optimizing n_r and n_i and permitting the switch-point to vary around the initial location. The theoretical AM fits in the non-TIR and TIR regimes do not match continuously, resulting in a spike (bold blue curves in Figs. 2). Clearly, the spike is an unavoidable artifact of our AM-fitting procedure and does not show up in the data or, indeed, in traditional F theory, which treats n_i the same (constant) through both TIR and non-TIR regimes. However, while our AM model may be outperformed by F theory in fitting 20 datapoints that span a small fraction of the murky transition region between TIR and non-TIR (see bottom inset, Fig. 2), the AM fit is unprecedentedly excellent over the remaining 1000 datapoints.

We believe that slight errors in the weight in grams of polystyrene spheres per 100 ml of colloidal solution quoted to us by the manufacturer (this number is converted to a volume-fraction% by dividing by the density of polystyrene) is one contributing factor to the residual discrepancy of under 10% between the particle sizes measured by our AM method relative to DLS. These errors would also contribute to the slight, but significant, difference in particle sizes measured by our AM method for different concentrations of the same particle. For example, an error bar of ±5% in the concentrations quoted by the manufacturer would lead to an error of ±4.5% in the particle size extracted for the two 0.5 μm solutions by our method and an error of ±2.5% for the three 0.2 μm solutions. Another possible factor that contributes to the residual discrepancy in particle size measurement by AM versus DLS is that there may be slight changes in the refractive index measured by the AM method owing to density gradients forming at the glass interface due to the colloidal particles developing slightly charged surfaces. Of course, the size extracted by the DLS method on the Zetasizer is independent of concentration; hence the DLS particle sizes are identical.

In conclusion, we have demonstrated a verifiably accurate methodology for *in situ* particle sizing and complex refractive index measurement of highly turbid media.

Funding from Petroleum Research Fund and Dillon-Kane, LLC, is gratefully acknowledged. We thank Miami University's Instrumentation Lab for help with Labview. We are grateful to three anonymous referees whose insightful suggestions contributed immensely to this Letter.

References and Notes

1. S. Faez, P. M. Johnson, and A. Lagendijk, Phys. Rev. Lett. **103**, 053903 (2009).
2. W. Calhoun, H. Maeta, A. Combs, L. Bali, and S. Bali, Opt. Lett. **35**, 1224 (2010).
3. W. Calhoun, H. Maeta, A. Combs, L. Bali, and S. Bali, Opt. Lett. **36**, 3172 (2011).
4. G. Meeten and A. North, Meas. Sci. Technol. **6**, 214 (1995).
5. I. Niskanen, J. Räty, and K. Peiponen, Opt. Lett. **32**, 862 (2007).
6. G. Meeten, Meas. Sci. Technol. **8**, 728 (1997).
7. A. Garcia-Valenzuela, R. Barrera, C. Sanchez-Perez, A. Reyes-Coronado, and E. Mendez, Opt. Express **13**, 6723 (2005).
8. W. Guo, M. Xia, W. Li, J. Dai, and K. Yang, Rev. Sci. Instrum. **82**, 053108 (2011).
9. W. Guo, M. Xia, W. Lei, J. Dai, X. Zhang, and K. Yang, Meas. Sci. Technol. **23**, 047001 (2012).
10. S. A. Prahl, http://omlc.ogi.edu/calc/mie_calc.html.
11. N. Ren, J. Liang, X. Qu, J. Li, B. Lu, and J. Tian, Opt. Express **18**, 6811 (2010).
12. K. Goyal, M. Dong, D. Kane, S. Makkar, B. Worth, L. Bali, and S. Bali, Rev. Sci. Instrum. **83**, 086107 (2012).
13. M. McClimans, C. LaPlante, D. Bonner, and S. Bali, Appl. Opt. **45**, 6477 (2006).
14. C. A. Risset and J. M. Vigoureaux, Opt. Commun. **91**, 155 (1992).
15. K. H. Lan, N. Ostrowsky, and D. Sornette, Phys. Rev. Lett. **57**, 17 (1986).
16. H. Matsuoka, Macromol. Rapid Commun. **22**, 51 (2001).
17. V. Kontturi, P. Turunen, J. Uozumi, and K. Peiponen, Opt. Lett. **34**, 3743 (2009).
18. M. A. C. Potenza, D. Brogioli, and M. Giglio, Appl. Phys. Lett. **85**, 2730 (2004).
19. D. Huh, J. Bahng, Y. Ling, H. Wei, O. Kripfgans, J. Fowlkes, J. Grotberg, and S. Takayama, Anal. Chem. **79**, 1369 (2007).
20. Alternatively one may use manufacturer provided values based on dry microscopy. Our conclusions are unaltered.
21. X. Ma, J. Lu, R. Brock, K. Jacobs, P. Yang, and X. Hu, Phys. Med. Biol. **48**, 4165 (2003).